Thornber, J. P. (1971) *Methods Enzymol. 23*, 688-691.
Thornber, J. P. (1986) *Encycl. Plant Physiol., New Ser. 19*, 85-142.
van Grondelle, R., Bergstrom, H., Sundstrom, V., van Dorssen, R. J., Vos, M., & Hunter, C. N. (1988) in *Structure and Function in Photosynthetic Light Harvesting Systems* (Scheer, H., & Schneider, S., Eds.) pp 519-530, Walter De Gruyter, Berlin.
Won, Y., & Friesner, R. A. (1988) *Isr. J. Chem. 28*, 67-72.
Zuber, H. (1985) *Photochem. Photobiol. 42*, 821-844.
Zuber, H., Brunisholz, R., & Sidler, W. (1987) *New Compr. Biol. 15*, 233-272.

# Fluorescence of Tryptophan Dipeptides: Correlations with the Rotamer Model

Raymond F. Chen,*,‡ Jay R. Knutson,‡ Herman Ziffer,§ and Denise Porter‡
*Laboratory of Cellular Biology, National Heart, Lung, and Blood Institute, National Institutes of Health, Bethesda, Maryland 20892, and Laboratory of Chemical Physics, National Institute of Diabetes and Digestive and Kidney Diseases, National Institutes of Health, Bethesda, Maryland 20892*
*Received August 1, 1990; Revised Manuscript Received February 26, 1991*

ABSTRACT: The multiexponential decay of tryptophan derivatives has previously been explained by the presence of rotamers having different fluorescence lifetimes, but it has been difficult to correlate rotamer structure and physical properties. New time-resolved and static data on dipeptides of the type Trp-X and X-Trp, where X is another aminoacyl residue, are consistent with the rotamer model and allow some correlations. That a dominant rotamer of Trp-X zwitterion has the $-NH_3^+$ group near the indole ring was inferred from absorption and fluorescence spectra, titrimetric determination of $pK_a$ values, photochemical hydrogen–deuterium-exchange experiments, decay-associated spectra, quantum yields, and decay kinetics. Analysis of the lifetime and quantum yield data for Trp dipeptides, especially X-Trp, suggests that static self-quenching is not uncommon. Highly quenched and weak components of the fluorescence do not contribute to the calculated mean lifetime, thus resulting in apparent static quenching. We propose the term *quasi-static self-quenching* (QSSQ) to distinguish this phenomenon from quenching due to ground-state formation of a dark complex. Mechanisms of quenching and the structure of statically quenched rotamers are discussed. The occurrence of QSSQ supports the idea that rotamers interconvert slowly. A major perceived deficiency of the rotamer model, namely, the apparent inability to predict reasonable rotamer populations from fluorescence decay data, may result from the presence of statically quenched species, which do not contribute to the fluorescence.

The idea that different conformations of a given protein coexist in solution has been supported by fluorescence decay measurements. The fluorescence decay of a single species should be monoexponential [e.g., Pringsheim (1949)], so it might be supposed that proteins having a single tryptophan responsible for their fluorescence should each have monoexponential decay. However, most such proteins exhibit multiexponential behavior (DeLauder & Wahl, 1971; Conti & Forster, 1975; Formoso & Forster, 1975; Grinvald & Steinberg, 1976), suggesting the presence of conformers. Tryptophan, its derivatives, and other indole-containing compounds have often been used as models for the study of protein fluorescence. Many of these compounds exhibit nonexponential decay, in analogy with that of single-tryptophan proteins. Rayner and Szabo (1978) first showed that tryptophan zwitterion had biexponential decay kinetics, and others have noted that the decays of tryptophan derivatives were multiexponential (Werner & Forster, 1979; Petrich et al., 1983). Similar nonexponential decay has been noted for tyrosine and related compounds (Gauduchon & Wahl, 1978; Ross et al., 1986; Laws et al., 1986).

These phenomena are most easily explained on the basis of the presence of several conformers, each with different fluorescence lifetimes. In the case of aromatic amino acids, these conformers are postulated to be formed by rotation of carbons about the $C_\alpha$–$C_\beta$ and/or $C_\beta$–$C_\gamma$ bonds (Donzel et al., 1974; Szabo & Rayner, 1980; Robbins et al., 1980; Ross et al., 1981). Attempts have been made (Szabo & Rayner, 1980; Petrich et al., 1983; Gudgin-Templeton & Ware, 1984; Beechem & Brand, 1985) to correlate lifetime components with rotamer populations inferred from NMR measurements (Dezube et al., 1981).

Investigation of the rotamer model is clearly desirable for an understanding of protein fluorescence kinetics. Here, we report spectral and lifetime data for tryptophan dipeptides of the form Trp-X and X-Trp, where X is another amino acid, to see if the properties fit the rotamer model. We provide evidence that a single rotamer predominates in Trp-X dipeptides, in which the indole and amino groups are close and influence each other's properties. Quantum yield and lifetime data show that X-Trp zwitterions regularly exhibit static self-quenching. Evidence for such static quenching has been sought unsuccessfully in the past, possibly due to poor precision in lifetime and quantum yield measurements. These findings have interesting implications for the interpretation of protein fluorescence.

## Materials and Methods

Peptides were obtained from the following sources: Trp-Val and Trp-β-Ala were from U.S. Biochemical Corp. Trp-Lys, Tyr-Trp, Glu-Trp, and Lys-Trp were from Research Plus, Inc. Gly-Trp-Gly, Trp-Ser, and Phe-Trp were obtained from

* To whom correspondence should be addressed.
‡ National Heart, Lung, and Blood Institute.
§ National Institute of Diabetes and Digestive and Kidney Diseases.

Chemical Dynamics Corp. Gly-Gly-Trp, Trp-Leu, and Trp-Gly-Gly were obtained from Vega. *N,N,N*-Trimethyltryptophan was a gift of Dr. James M. Cook, University of Wisconsin. *N*-Methyltryptophan (L-abrine) was purchased from Aldrich Chemical Co. All other peptides and melatonin, 5-methoxy-*N*-acetyltryptamine, were obtained from Sigma Chemical Co. The purity of the compounds was checked by HPLC (Hewlett-Packard Model 1084) and paper chromatography with ninhydrin spray visualization.

Absorption spectra were recorded on a Cary spectrophotometer. Static fluorescence measurements were performed with ISS and Aminco-Bowman spectrofluorometers. Relative quantum yields, $Q_{rel}$, were obtained by the comparative method (Parker & Rees, 1960), with use of tryptophan zwitterion as a standard of quantum yield 1.0. Because all compounds examined had nearly identical excitation and emission spectra, it was assumed that the quantum yields were proportional to the intensity of fluorescence at 350 nm measured with a 12-nm band-pass. The optical densities were measured at 279 nm, the excitation wavelength; and solution concentrations were adjusted to give optical densities below 0.10. Small corrections were applied for self-absorption (Chen et al., 1969). Fluorescence titrations of peptides were performed by first dissolving the compounds in 0.001 M potassium phosphate, pH 7, adjusting the pH with 1 M HCl or KOH, and reading the fluorescence after each addition. Corrections for volume change were negligible.

Photochemical hydrogen–deuterium-exchange experiments were conducted with a water-cooled, 450-W Hanovia high-pressure xenon arc lamp. Tryptophan and tryptophanyl peptide samples were dissolved in $D_2O$ and the pH was adjusted with DCl. Solutions were placed in thin pyrex NMR tubes, placed 4 cm from the arc, and exposed for 30 min. Saito et al. (1984) described hydrogen–deuterium exchange at the C-4 of tryptophan under similar conditions. Their result was duplicated with this configuration, but exchange was blocked with the addition of a 2-mm pyrex shield. The samples were analyzed by use of a Varian 200-MHz NMR spectrometer.

Time-resolved fluorescence data were obtained with a single-photon counting apparatus used previously (Chen & Knutson, 1988). The doubled output of a Spectra-Physics Series 3000 mode-locked, cavity-dumped Nd:YAG laser synchronously pumps a tunable dye laser (Spectra Physics 3500) whose output is doubled into the ultraviolet. For the present work, rhodamine 6G was the laser dye used, and magic angle excitation was employed at 295 nm with pulses having a FWHM of 10–13 ps. The fluorescence was recorded at 350 nm in the time-correlated, single-photon mode, by use of a cooled HR955S photomultiplier. The instrumental response width was 800 ps, so that measurement of lifetimes of 150 ps or greater could be made with use of conventional deconvolution. Fluorescence with a much shorter lifetime would be detected but would have the same shape as the excitation pulses except for occurring at emission wavelengths. A JYH10 monochromator was used to select the emission. For decay analysis of tryptophan derivatives at a single emission wavelength, fluorescence was detected through a pyrex filter with the monochromator set at 350 nm with an 8-nm bandwidth.

The phototube transit time dependence on wavelength ("color shift") may introduce a small error (Ware & Nemzek, 1975). With 295 nm and 350 nm excitation and emission, the time base correction that was required was normally less than one channel (set at 88 ps/channel) of the multichannel analyzer. Melatonin in water at 23 °C was used as a standard, for which separate experiments showed monoexponential decay and a lifetime of 5.4 ns. A deviation from monoexponential decay was signaled by an $\chi^2$ that is improved by fitting to a multiexponential model, and this was assumed to be due to phototube color shift. The correction consisted of insertion of the minimum time shift required to make the melatonin data consistent with monoexponential decay.

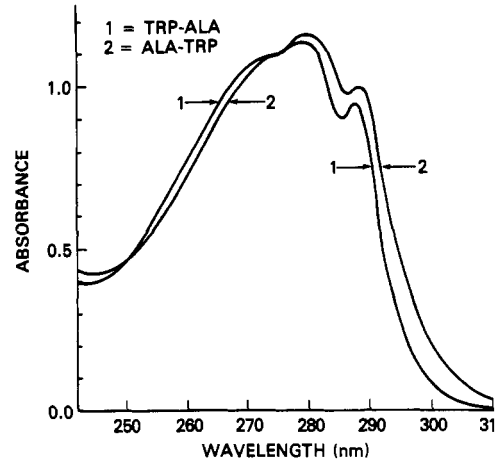


FIGURE 1: Absorption spectra of Trp-Ala and Ala-Trp zwitterions, pH 5.5.

Lifetimes were obtained by fitting the decay data to a triple-exponential model, according to the weighted, least-squares method (Grinvald & Steinberg, 1974). Goodness of fit was assessed with the $\chi^2$ function [see Badea and Brand (1979)]. The fits for which data are given in the tables yielded values of 1.1–1.6. In the tables of lifetimes in this paper, where the results of a triple-exponential analysis yielded components with very small amplitudes, a single- or double-exponential model would have yielded a satisfactory fit.

For decay-associated spectra (DAS; Knutson et al., 1982), time-resolved data were obtained on tryptophanyl peptides by excitation at 296 nm and observation every 5 nm over the emission band. The exciting light profile was obtained with a light-scattering suspension (Ludox, Dupont de Nemours Co.). Alternating the sample with the scatterer, stepping of the emission monochromator, data collection, and transfer of data from the multichannel analyzer to the minicomputer (Hewlett-Packard A900) were done automatically through a program developed by Janet White, Biomedical Engineering and Instrumentation Branch, National Institutes of Health. In the analysis of the multiple curves obtained for a DAS, they were all fit to the same triple-exponential model ("global analysis"; Knutson et al., 1983).

## Results

(*1*) *Absorption Spectra.* The tryptophan peptides studied here all showed typical indole absorption in water, with a peak near 279 nm. When the absorption spectra of dipeptide pairs Trp-X and X-Trp were examined, it was noted that the spectrum of the Trp-X zwitterion was blue-shifted relative to the spectrum of its anion, which in turn was essentially identical with the spectra of the X-Trp anion and zwitterion The spectra for Trp-Ala and Ala-Trp zwitterions are given in Figure 1. This absorption blue shift of the zwitterion was noted for tryptophan itself by Hermans et al. (1960), for several Trp peptides by Wiget and Luisi (1978), and for Trp, Trp-Gly, and Trp-Ala by Chang et al. (1983). The spectra of the Trp-Ala and Ala-Trp zwitterions are compared in Figure 1. We have examined similar spectra for all the Trp-X and X-Trp pairs listed in our tables, and we find that the blue shift is a general feature of the Trp-X zwitterions. On the other

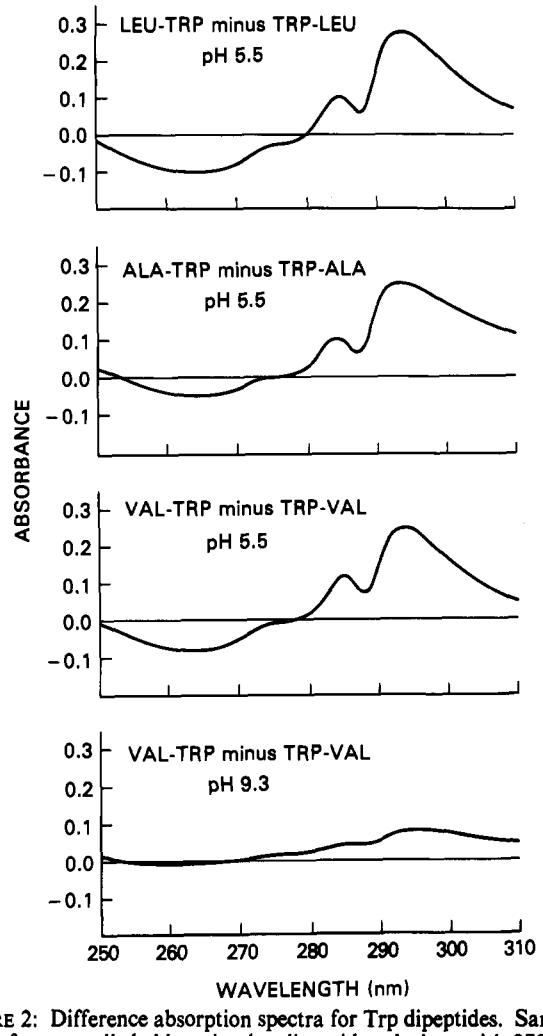


FIGURE 2: Difference absorption spectra for Trp dipeptides. Sample and reference cells held equimolar dipeptide solutions with 279-nm absorbance maxima ~ 1.15, as in Figure 1.

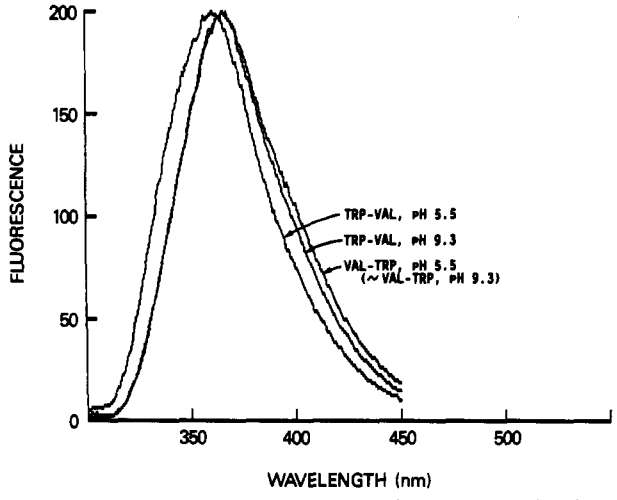


FIGURE 3: Emission spectra (uncorrected) for Trp-Val and Val-Trp. The peak for the zwitterion of Trp-Val (pH 5.5) is shifted by 9.5 nm to the blue.

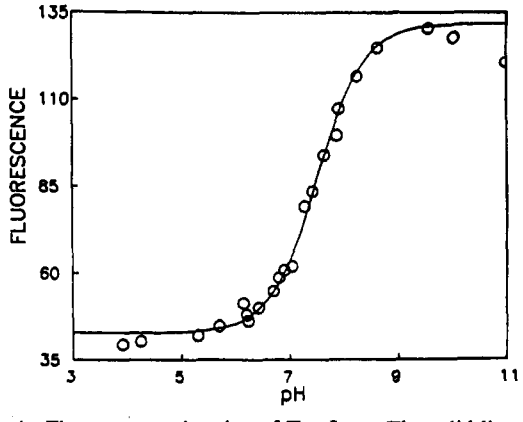


FIGURE 4: Fluorescence titration of Trp-Leu. The solid line is the fit of eq 1 (see text) to the experimental points (O) in the range of pH 5–9. The calculated p$K_a$ is 7.51.

hand, the spectra of the X-Trp anions and zwitterions are very similar. Chang et al. (1983) reported that Gly-Trp and Ala-Trp showed no shift, whereas Wiget and Luisi (1978) reported that the emission peak of Gly-Trp shifted from 355 to 354 nm, in converting the anion to the zwitterion. As shown in Figure 1, the zwitterionic blue shift is represented by a small 2–3-nm shift in absorption maximum plus a corresponding overall shift of the long wavelength band. Neither Chang et al. (1983) nor we observed the 12-nm difference between the absorption maxima of Trp-Gly anion and zwitterion reported by Wiget and Luisi (1978). These changes were more extensively identified through difference spectra as shown in Figure 2. These data illustrate the finding that the blue shifts are the same for each dipeptide pair and that at pH 9.3, where the anionic forms predominate, there is little difference in spectra of Trp-X and X-Trp. The largest difference in the zwitterion spectra occurs at 294 nm, a wavelength used by Chang et al. (1983) to determine the p$K_a$ of tryptophan, Trp-Gly, and Trp-Ala by spectrophotometric titration. Unlike their results showing two isosbestic points for Trp-Gly above 260 nm, we find only one isosbestic point above 260 nm as shown by the zero-point crossing at 275–278 nm in the difference spectra shown in Figure 2.

The blue shift of Trp-X zwitterion is also seen in the emission spectrum as shown for Trp-Val in Figure 3.

Since the identity of X does not seem to affect the spectra, the blue shift is probably entirely due to changes occurring in the tryptophanyl moiety, namely, charge interaction between the indole ring and the amino group.

*(2) Effect of Tryptophan Position on the p$K_a$ of Dipeptides.* The p$K_a$ values of the $-NH_3^+$ groups of Trp-X and X-Trp were determined by fluorometric titration, on the basis of the fact that the anion has higher quantum yield than the zwitterion. Although it has been shown that the difference absorption band at 275–278 nm can be used to determine the p$K_a$ by use of spectrophotometric titration (Chang et al., 1983), there is no usable difference between the absorption spectra of anionic and zwitterionic X-Trp dipeptides. A typical fluorometric titration is shown for Trp-Leu in Figure 4. The data were fit to the expression

$$F = (\exp(-2.303\mathrm{pH})(F_N - D) + (K_a F_N))/((\exp(-2.303\mathrm{pH}) + K_a)) \quad (1)$$

where $F$ is the fluorescence intensity at a given pH, $F_N$ is the fluorescence of the anionic form, $D$ is the difference between the intensities of the anionic and zwitterionic forms, and $K_a$ is the dissociation constant. There is some uncertainty as to the values of $F_N$ and $D$ for two reasons: at high pH, quenching by hydroxyl ion may obscure the plateau region where the anion predominates, while at low pH, a further decrease in fluorescence due to the protonation of the carboxyl group overlaps the plateau region of the zwitterion. However, by treating not only $K_a$ but also $F_N$ and $D$ as variables in the fitting procedure and discarding points at extremes of pH, it was possible to obtain excellent fits to the data with p$K_a$ values that agreed well with those in the literature, where available.

Table I: $pK_a$ Values for Tryptophan Peptides

| | |
|---|---|
| Ala-Trp | 7.82 |
| Trp-Ala | 7.32 |
| β-Ala-Trp | 9.08 |
| Trp-β-Ala | 7.44 |
| Gly-Trp | 7.93 |
| Trp-Gly | 7.53 |
| Gly-Gly-Trp | 7.55 |
| Trp-Gly-Gly | 7.17 |
| Leu-Trp | 7.51 |
| Trp-Leu | 7.19 |
| Phe-Trp | 6.75 |
| Trp-Phe | 6.92 |
| Trp-Trp | 7.18 |
| Val-Trp | 7.54 |
| Trp-Val | 7.26 |
| Pro-Trp | 8.30 |
| Trp-Ser | 7.06 |

The results of these measurements are shown in Table I. Several features should be noted: First, the $pK_a$ values are generally considerably lower than those for aliphatic amines, which normally fall in the region of 9.5. Second, for each pair, with one exception, the peptide with N-terminal Trp has the lower $pK_a$. An explanation of these results is that the hydrophobicity of the indole moiety favors loss of a proton from the charged amino groups, which is closer to the indole in N-terminal Trp peptides but able to affect the $pK_a$ even in X-Trp dipeptides. In the case of β-Ala-Trp, and $pK_a$ of 9.04 reflects the greater average distance between indole and amino groups. Only in the case of Phe-Trp is the $pK_a$ of an X-Trp dipeptide lower than that of the corresponding Trp-X. This can be rationalized in terms of the lower polarity of the phenyl group relative to the indole. These results again suggest proximity of the amino group and the side chain of the N-terminal residue.

(3) *Fluorescence Decay Kinetics.* The decay curves of anionic and zwitterionic forms of Trp peptides were obtained by use of excitation at 296 nm and emission at 350 nm. The results showed a pattern in which Trp-X anion fluorescence decay was nearly monoexponential and that of X-Trp zwitterion anion was grossly nonexponential, while Trp-X zwitterion and X-Trp anion decays were moderately nonexponential. The length of the lifetimes also fit a pattern, namely, Trp-X anion > X-Trp anion > Trp-X zwitterion > X-Trp zwitterion. Typical data, those for Trp-Leu and Leu-Trp, are shown in Figure 5A,B, from which the general form of the decay curves can be seen even before deconvolution. The data analyses routinely included deconvolution for the excitation pulse, which had an instrumental FWHM of 800 ps (a typical pulse was shown previously; Chen & Knutson, 1988). The decay data, $I'(t)$, were analyzed according to a convolved triple-exponential model

$$I'(t) = \int L(t)\, I(t' - t)\, dt \qquad (2)$$

where $L(t)$ is the lamp function and

$$I(t) = I_0(\alpha_1 e^{-t/\tau_1} + \alpha_2 e^{-t/\tau_2} + \alpha_3 e^{-t/\tau_3})$$

Here, $I(t)$ and $I_0$ are the intensities at time $t$ and $t = 0$, $\alpha_i$ is the preexponential such that $\sum\alpha_i = 1$, and $\tau_i$ are the lifetimes. The results are summarized in Tables II and III. Also included are the mean lifetimes, namely, the intensity-weighted lifetime $\tau_m$ and the species-concentration-weighted lifetime $\langle\tau\rangle$, defined as

$$\tau_m = \frac{\sum\alpha_i\tau_i^2}{\sum\alpha_i\tau_i}$$

and

$$\langle\tau\rangle = \sum\alpha_i\tau_i$$

The mean lifetimes at a given pH were always longer for

Table II: Lifetime Data for Trp-X Peptides[a]

| peptide | $\alpha_1$ | $\tau_1$ | $I_1$% | $\alpha_2$ | $\tau_2$ | $I_2$% | $a_3$ | $\tau_3$ | $I_3$% | $\tau_m$ | $\langle\tau\rangle$ |
|---|---|---|---|---|---|---|---|---|---|---|---|
| | | | | | at pH 5.5 | | | | | | |
| Trp-Ala | 0.65 | 1.76 | 85.7 | 0.34 | 0.31 | 7.9 | 0.01 | 6.47 | 6.5 | 1.94 | 1.33 |
| Trp-β-Ala | 0.20 | 0.48 | 5.7 | 0.79 | 1.88 | 88.9 | 0.01 | 6.41 | 5.5 | 2.05 | 1.67 |
| Trp-Glu | 0.71 | 1.95 | 82.5 | 0.28 | 0.73 | 12.3 | 0.01 | 7.22 | 5.2 | 2.07 | 1.67 |
| Trp-Gly | 0.28 | 0.39 | 7.8 | 0.70 | 1.63 | 82.6 | 0.22 | 6.18 | 9.6 | 1.97 | 1.38 |
| Trp-Gly-Gly | 0.34 | 1.42 | 47.8 | 0.62 | 0.53 | 32.2 | 0.04 | 5.02 | 20.0 | 1.86 | 1.02 |
| Trp-Leu | 0.67 | 2.12 | 62.6 | 0.21 | 0.61 | 5.7 | 0.12 | 5.849 | 31.8 | 3.22 | 2.26 |
| Trp-Lys | 0.48 | 1.82 | 77.2 | 0.51 | 0.14 | 6.9 | 0.02 | 5.80 | 15.9 | 2.33 | 1.08 |
| Trp-Phe | 0.46 | 0.87 | 24.8 | 0.51 | 1.97 | 63.2 | 0.03 | 7.35 | 12.0 | 2.34 | 1.60 |
| Trp-Trp | 0.58 | 0.68 | 35.4 | 0.39 | 1.62 | 57.3 | 0.02 | 3.52 | 7.3 | 1.43 | 1.12 |
| Trp-Tyr | 0.39 | 2.74 | 52.8 | 0.57 | 1.28 | 35.6 | 0.04 | 5.99 | 11.6 | 2.60 | 2.04 |
| Trp-Val | 0.43 | 0.27 | 8.5 | 0.50 | 1.71 | 63.7 | 0.07 | 5.10 | 27.8 | 2.53 | 1.34 |
| Trp-Ser | 0.59 | 1.58 | 65.8 | 0.36 | 0.48 | 12.1 | 0.06 | 5.22 | 22.1 | 2.25 | 1.41 |
| NAcTrp | 0.10 | 0.98 | 2.4 | 0.70 | 4.34 | 72.4 | 0.20 | 5.28 | 25.2 | 4.49 | 4.18 |
| | | | | | at pH 9.3 | | | | | | |
| Trp-Ala | 0.05 | 2.33 | 1.8 | 0.03 | 0.25 | 0.5 | 0.92 | 7.29 | 97.8 | 7.17 | 6.80 |
| Trp-β-Ala | 0.08 | 1.69 | 2.0 | 0.77 | 6.90 | 77.7 | 0.16 | 8.97 | 20.4 | 7.22 | 6.81 |
| Trp-Glu | 0.20 | 1.35 | 4.4 | 0.66 | 6.79 | 71.6 | 0.15 | 10.17 | 23.9 | 7.35 | 6.21 |
| Trp-Gly | 0.18 | 0.24 | 0.08 | 0.81 | 6.63 | 95.6 | 0.01 | 16.73 | 3.6 | 6.95 | 5.60 |
| Trp-Gly-Gly | 0.22 | 1.12 | 6.1 | 0.78 | 4.73 | 93.9 | | | | 4.51 | 3.95 |
| Trp-Leu | 0.09 | 1.28 | 1.9 | 0.39 | 5.49 | 33.9 | 0.52 | 7.74 | 64.2 | 6.86 | 6.28 |
| Trp-Lys | 0.16 | 1.27 | 3.5 | 0.66 | 6.27 | 70.7 | 0.18 | 8.37 | 25.9 | 6.65 | 5.87 |
| Trp-Phe | 0.15 | 0.70 | 1.7 | 0.66 | 6.44 | 71.8 | 0.19 | 8.43 | 26.5 | 6.87 | 5.96 |
| Trp-Trp | 0.21 | 1.04 | 8.0 | 0.78 | 3.10 | 89.2 | 0.01 | 7.11 | 2.8 | 3.05 | 2.71 |
| Trp-Tyr | 0.39 | 2.69 | 22.1 | 0.60 | 5.76 | 73.9 | 0.01 | 13.68 | 4.0 | 5.40 | 4.69 |
| Trp-Val | 0.48 | 7.47 | 97.2 | 0.42 | 0.01 | 0.06 | 0.10 | 1.04 | 2.7 | 7.29 | 3.72 |
| Trp-Ser | 0.20 | 0.65 | 2.3 | 0.31 | 5.09 | 28.0 | 0.49 | 7.89 | 69.7 | 6.94 | 5.58 |
| NAcTrp | 0.14 | 2.76 | 8.5 | 0.86 | 4.74 | 91.5 | | | | 4.56 | 4.47 |

[a] $\alpha_i$, $\tau_i$, and $I_i$ are the preexponentials, lifetimes in nanoseconds, and percent of the total intensity associated with component $i$. $\tau_m$ and $\langle\tau\rangle$ are the mean lifetimes as defined in the text.

Table III: Lifetime Data for X-Trp Peptides[a]

| peptide | $\alpha_1$ | $\tau_1$ | $I_1$% | $\alpha_2$ | $\tau_2$ | $I_2$% | $a_3$ | $\tau_3$ | $I_3$% | $\tau_m$ | $\langle\tau\rangle$ |
|---|---|---|---|---|---|---|---|---|---|---|---|
| | | | | | at pH 5.5 | | | | | | |
| Ala-Trp | 0.43 | 0.44 | 19.9 | 0.55 | 1.28 | 73.9 | 0.02 | 3.64 | 6.2 | 1.26 | 0.95 |
| β-Ala-Trp | 0.72 | 1.36 | 57.6 | 0.28 | 2.51 | 41.6 | 0.01 | 22.23 | 0.8 | 2.00 | 1.82 |
| Glu-Trp | 0.46 | 1.94 | 59.7 | 0.52 | 1.03 | 36.1 | 0.01 | 3.80 | 4.3 | 1.69 | 1.50 |
| Gly-Trp | 0.54 | 1.15 | 75.6 | 0.46 | 0.41 | 23.0 | 0.00 | 3.36 | 1.4 | 0.98 | 0.81 |
| Gly-Gly-Trp | 0.45 | 1.26 | 57.6 | 0.44 | 0.46 | 20.5 | 0.10 | 2.09 | 21.8 | 1.28 | 1.00 |
| Leu-Trp | 0.57 | 0.92 | 32.3 | 0.43 | 2.51 | 66.5 | 0.01 | 19.93 | 1.2 | 2.21 | 1.88 |
| Lys-Trp | 0.62 | 1.70 | 70.0 | 0.34 | 0.88 | 20.1 | 0.04 | 3.79 | 9.9 | 1.74 | 1.50 |
| Phe-Trp | 0.48 | 0.34 | 15.1 | 0.43 | 1.45 | 58.2 | 0.10 | 3.01 | 26.8 | 1.70 | 1.07 |
| Pro-Trp | 0.41 | 0.25 | 12.9 | 0.54 | 1.09 | 73.3 | 0.05 | 2.27 | 13.8 | 1.14 | 0.88 |
| Trp-Trp | 0.58 | 0.68 | 35.4 | 0.39 | 1.62 | 57.3 | 0.02 | 3.52 | 7.3 | 1.43 | 1.12 |
| Tyr-Trp | 0.91 | 1.44 | 79.9 | 0.09 | 3.48 | 19.8 | 0.00 | 4.99 | 0.3 | 1.86 | 1.63 |
| Val-Trp | 0.41 | 1.47 | 51.2 | 0.51 | 0.29 | 23.5 | 0.08 | 5.18 | 36.3 | 2.67 | 1.18 |
| Ala-Trp | 0.24 | 0.68 | 7.2 | 0.75 | 2.74 | 91.6 | 0.01 | 1.37 | 1.2 | 2.58 | 2.20 |
| | | | | | at pH 9.3 | | | | | | |
| β-Ala-Trp | 0.41 | 1.61 | 21.0 | 0.59 | 4.06 | 76.3 | 0.01 | 11.06 | 2.7 | 3.73 | 3.11 |
| Glu-Trp | 0.476 | 4.22 | 59.7 | 0.53 | 2.38 | 38.3 | | 16.9 | 2.0 | 3.77 | 3.29 |
| Gly-Trp | 0.42 | 0.61 | 18.5 | 0.58 | 1.89 | 80.7 | 0.01 | 10.72 | 0.9 | 1.73 | 1.50 |
| Gly-Gly-Trp | 0.59 | 1.63 | 69.0 | 0.34 | 0.60 | 14.5 | 0.08 | 3.06 | 16.6 | 1.71 | 1.39 |
| Leu-Trp | 0.57 | 1.21 | 5.4 | 0.79 | 4.09 | 85.7 | 0.04 | 8.46 | 8.9 | 4.32 | 4.26 |
| Lys-Trp | 0.15 | 0.66 | 3.3 | 0.72 | 3.04 | 72.7 | 0.12 | 5.92 | 24.0 | 3.65 | 3.03 |
| Phe-Trp | 0.17 | 0.62 | 3.7 | 0.40 | 2.61 | 35.8 | 0.43 | 4.08 | 60.6 | 3.43 | 2.89 |
| Pro-Trp | 0.11 | 0.67 | 1.4 | 0.29 | 3.03 | 16.0 | 0.60 | 7.07 | 81.9 | 6.30 | 5.21 |
| Trp-Trp | 0.21 | 1.04 | 8.0 | 0.78 | 3.10 | 89.2 | 0.01 | 7.11 | 2.8 | 3.05 | 2.71 |
| Tyr-Trp | 0.56 | 3.24 | 72.2 | 0.43 | 1.52 | 26.3 | 0.01 | 11.9 | 1.61 | 2.92 | 2.51 |
| Val-Trp | 0.16 | 1.19 | 4.1 | 0.70 | 5.10 | 75.5 | 0.14 | 7.01 | 20.4 | 5.33 | 4.73 |

[a] Symbols are as in Table II.

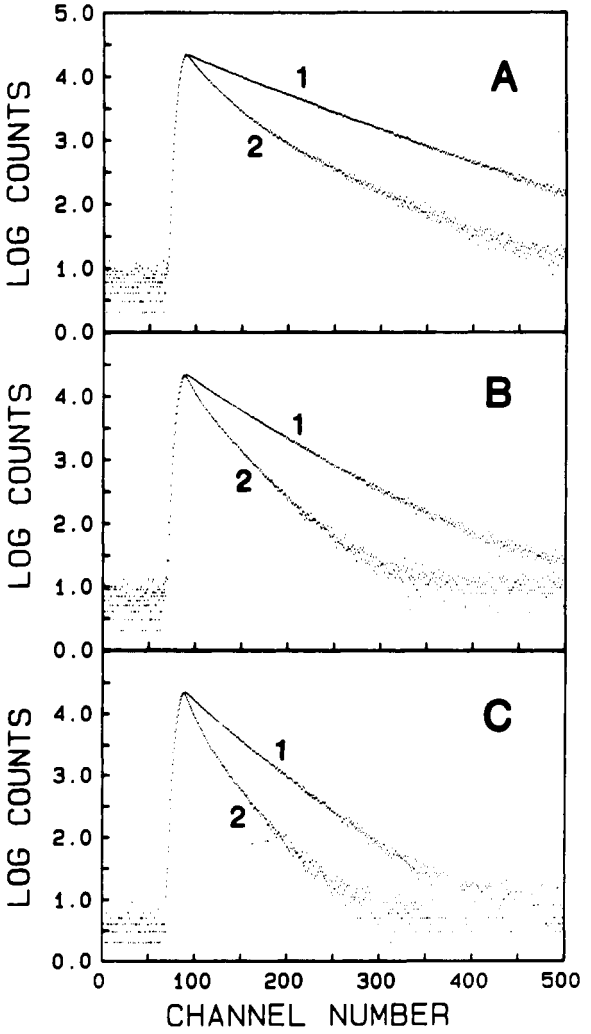


FIGURE 5: Fluorescence decay curves for Trp dipeptides: (A) Trp-Leu, (B) Leu-Trp, and (C) Trp-Trp. Excitation and emission: 295 nm and 350 nm. Data labeled 1 and 2 were obtained at pH 9.3 and 5.5, respectively.

Trp-X as opposed to X-Trp. The degree of departure from monoexponential decay can be assessed from the relative sizes of the preexponentials, the percent contribution to the intensity ($I_i$) of each component, and the difference between $\tau_m$ and $\langle\tau\rangle$. Where a decay is made up of components differing greatly in lifetime, $\tau_m$ will be much longer than $\langle\tau\rangle$.

In Table II, data for comparison are included for *N*-acetyltryptophan, whose decay is nearly monoexponential and whose lifetime of 4.5 ns is longer than that of free Trp zwitterion (3.10 ns; Raynor & Szabo, 1979).

In comparing data for the anions, X-Trp anions have mean lifetimes roughly half as long as those of Trp-X, which are approximately 6.7 ± 0.5 ns. At pH 5.5, where the zwitterions predominate, $\tau_m$ for Trp-X falls mostly in the range 2.5 ± 0.5 ns, while for X-Trp the value is about 1.7 ± 0.5 ns. Note in Table II, that the lifetime for Trp-Trp is typical for X-Trp rather than Trp-X. The lifetime data of Tables II and III are used in the calculations of Table IV and discussed further below.

(*4*) *Decay-Associated Spectra.* In complex systems, decay-associated spectra (DAS) are the emission spectra that are computationally related to the lifetimes obtained from fluorescence decay curves (Knutson et al., 1982). DAS are useful as an index of the degree of heterogeneity of the emission but do not, in themselves, specify their origin. Figure 6 gives the DAS for Trp-Ala and Ala-Trp. To obtain these DAS, decay curves were recorded every 5 nm through the emission band. The three lifetimes were obtained by fitting all the curves, rather than a single curve, to a three-exponential model. The DAS can then be viewed as plots of the preexponential constants at each wavelength, with the spectra then normalized with respect to percent intensity contribution. In each sector of Figure 6, the overall spectrum ($I_t$) is the sum of the other three curves. The spectrum of Ala-Trp zwitterion (pH 5.5) is clearly a composite of species having slightly different spectra. In contrast, the DAS of Trp-Ala anion is essentially that of a single component making up 98% of the intensity. While the DAS are crude compared with steady-

Table IV: Lifetimes/Quantum Yield Ratios[a]

| | pH 5.5 | | | pH 9.3 | | |
|---|---|---|---|---|---|---|
| compound | relative yield, $Q_{rel}$ | $\tau_m/Q_{rel}$ | $\langle\tau\rangle/Q_{rel}$ | relative yield, $Q_{rel}$ | $\tau_m/Q_{rel}$ | $\langle\tau\rangle/Q_{rel}$ |
| Ala-Trp | 0.298 | 4.23 | 3.20 | 0.969 | 3.50 | 2.27 |
| Trp-Ala | 0.731 | 2.66 | 1.82 | 2.61 | 2.75 | 2.61 |
| β-Ala-Trp | 0.595 | 3.36 | 3.06 | 1.13 | 3.32 | 2.75 |
| Trp-β-Ala | 0.725 | 2.82 | 2.30 | 2.73 | 2.62 | 2.49 |
| Glu-Trp | 0.482 | 3.51 | 3.11 | 1.11 | 3.40 | 2.96 |
| Trp-Glu | 0.640 | 3.24 | 2.61 | 2.75 | 2.67 | 2.26 |
| Gly-Trp | 0.277 | 3.65 | 2.92 | 0.578 | 2.99 | 2.59 |
| Trp-Gly | 0.644 | 3.06 | 2.14 | 2.26 | 3.08 | 2.48 |
| Gly-Gly-Trp | 0.358 | 3.57 | 2.79 | 0.508 | 3.37 | 2.74 |
| Trp-Gly-Gly | 0.481 | 3.86 | 2.12 | 1.43 | 3.16 | 2.76 |
| Leu-Trp | 0.413 | 5.35 | 4.55 | 1.08 | 3.97 | 3.94 |
| Trp-Leu | 0.776 | 4.14 | 2.91 | 2.30 | 2.98 | 2.73 |
| Lys-Trp | 0.396 | 4.43 | 3.79 | 1.01 | 3.63 | 3.00 |
| Trp-Lys | 0.564 | 4.13 | 1.91 | 2.13 | 3.12 | 2.76 |
| Phe-Trp | 0.348 | 4.89 | 3.07 | 0.997 | 3.44 | 2.90 |
| Trp-Phe | 0.635 | 3.69 | 2.52 | 2.09 | 3.28 | 2.85 |
| Pro-Trp | 0.226 | 5.05 | 3.89 | 1.32[b] | 4.76 | 3.95 |
| Val-Trp | 0.455 | 5.86 | 2.59 | 1.84 | 2.90 | 2.57 |
| Trp-Val | 0.714 | 3.55 | 1.87 | 2.66 | 2.74 | 1.40 |
| NAcTrp | 1.67 | 2.69 | 2.50 | 1.67 | 2.73 | 2.68 |
| Trp-Trp | 0.363 | 3.93 | 3.09 | 0.991 | 3.07 | 2.73 |
| TMT[c] | 1.12 | 2.59 | 2.59 | | | |
| [tryptophan | 1.00 | 3.10 | 3.09] | | | |

[a] All compounds were measured at 23 °C in 0.01 M sodium acetate, pH 5.5, or sodium borate, pH 9.3, buffers. The ratios are based on the $\tau_m$ and $\langle\tau\rangle$ values of Tables II and III. The yield, $Q_{rel}$, is relative to that of tryptophan at pH 7.0. The lifetime for tryptophan was calculated from the data of Rayner and Szabo (1978). [b] Measured at pH 10.0 [c] TMT = *N,N,N*-trimethyltryptophan.

state spectra, they demonstrate that the emission spectra of the major lifetime components of tryptophan dipeptides are similar though not identical. This finding is relevant to the question of whether different rotamers have differing radiative lifetimes (also known as natural lifetimes; see Discussion).

*(5) Quantum Yields, Static Quenching, and Quasi-Static Self-Quenching.* In order to gain insight into the mechanisms of quenching of Trp dipeptides, we measured the quantum yields and compared them with the fluorescence lifetimes. In dynamic quenching, where deactivation of the excited fluorophores is competitive with fluorescence

$$Q = \frac{\tau}{\tau_n} \qquad (3)$$

where $Q$ is the quantum yield, and $\tau_n$ is the natural, or radiative, lifetime that would be observed for $Q = 1$. Deviations from eq 3 such that $\tau/Q > \tau_n$ signify static quenching, which in turn is usually due to ground-state formation of nonfluorescent complexes. Equation 3 is therefore a guide to whether a quenching mechanism operates on the excited or ground state.

When applied to a heterogeneous solution, eq 3 should be modified to use a mean lifetime that is the sum of the contributions from each component, namely $\langle\tau\rangle$ (Werner & Forster, 1979). In this regard, the intensity-weighted lifetime $\tau_m$ is less correct but can be useful as described below. The quantum yields were measured relative to that of tryptophan zwitterion, $Q_{rel}$. Table IV shows the lifetime/quantum yield ratios for Trp peptides, expressed as both $\tau_m/Q_{rel}$ and $\langle\tau\rangle/Q_{rel}$. The latter ratio should be proportional to the natural lifetime and be constant in the absence of static quenching. However, with few exceptions, both ratios are higher for X-Trp than for Trp-X at a given pH. The difference is especially marked with the zwitterions (pH 5.5). The $\langle\tau\rangle/Q_{rel}$ value for Trp is 3.09, but the values for Leu-Trp, Lys-Trp, and Pro-Trp are significantly higher, suggesting the presence of intramolecular static quenching. This ratio is actually lower than 3.09 for many of the values shown in Table IV, suggesting that Trp zwitterion itself is not without static quenching. The values of $\langle\tau\rangle/Q_{rel}$ for *N*-acetyltryptophan and *N,N,N*-trimethyltryptophan are about 2.6, which is significantly lower than that of tryptophan and many dipeptides, especially X-Trp, listed in Table IV. This finding indicates that intramolecular static quenching may not be uncommon in these compounds. Note that the values that exceed 2.6 belong mainly to the X-Trp zwitterions (Table IV); of the anions listed, only Leu-Trp and Pro-Trp have values of $\langle\tau\rangle/Q_{rel} > 3.0$.

Several values of $\langle\tau\rangle/Q_{rel}$ for Trp-X dipeptides at pH 5.5 (Table IV) are anomalously low, even below 2. From the above considerations, one would not expect to find values of this ratio much below 2.6. The fact that these unexpectedly low ratios are found only for Trp-X dipeptides suggests that this is an artifact due to the presence of small amounts of the protonated species, which has a shorter lifetime than the zwitterion, since many of these dipeptides have $pK_a$ values near 7.0 (Table I). The concentration-weighted lifetime $\langle\tau\rangle$ is sensitive to such extraneous components, as explained below. In contrast, the ratios containing the intensity-weighted lifetime, namely, $\tau_m/Q_{rel}$, remain greater than 2.6.

The difference between $\tau_m$ and $\langle\tau\rangle$ is most markedly when there is a large disparity between lifetime components. For example, consider a two-component system where $\tau_2 \ll \tau_1$. As $\tau_2 \rightarrow 0$, $\langle\tau\rangle \rightarrow \alpha_1\tau_1$, whereas $\tau_m \rightarrow \tau_1$. At some point, the term $\alpha_2\tau_2$ becomes too small to be detected and $\langle\tau\rangle = \tau_m$. In this case, one component is effectively statically quenched, even though it may have a finite lifetime. This is admittedly an operational definition of static quenching, and an ideal lifetime fluorometer would detect all components. In a conventional

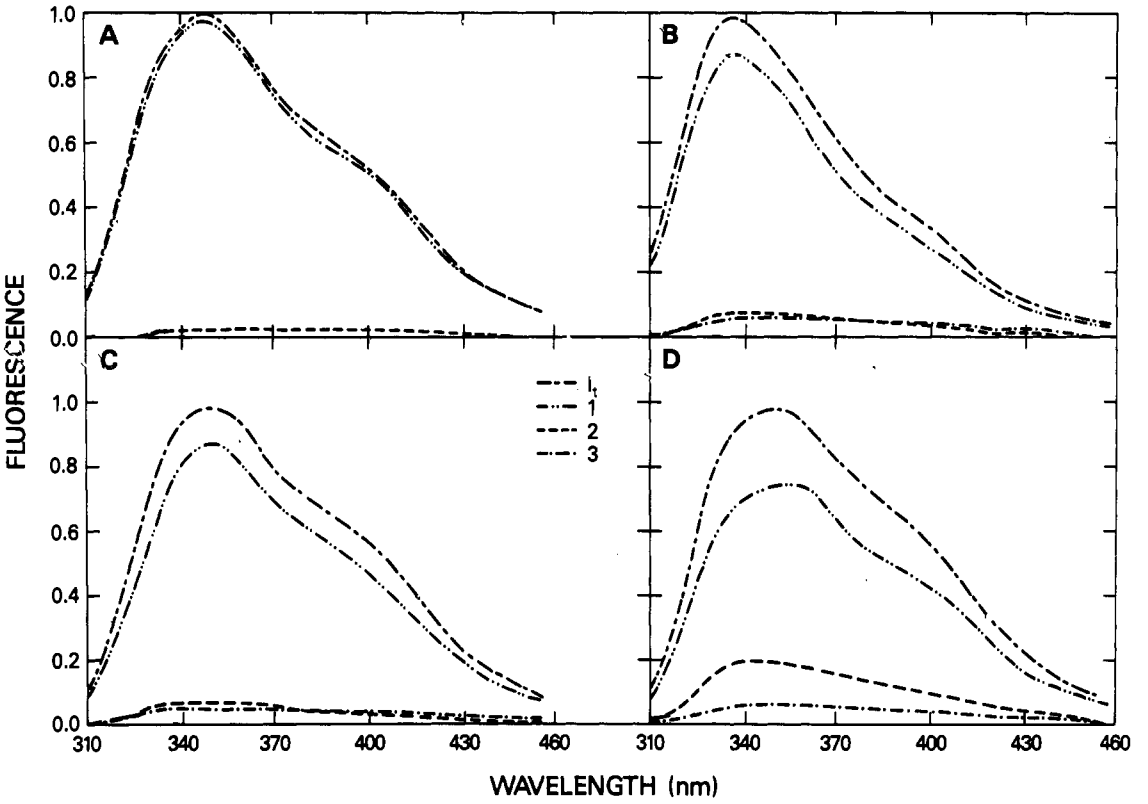


FIGURE 6: Decay-associated spectra for Trp-Ala and Ala-Trp. Decays were measured at 5-nm intervals and fitted to a triple-exponential model. Each panel contains four curves, three of which correspond to the lifetime components plotted in proportion to their intensities, and the other to the sum of the three, $I_t$. The legend key is given in panel C. The panels represent the following: (A) Trp-Ala anion (pH 9.3). Spectral components 1–3 correspond to 7.29, 2.33, and 0.925 ns. The latter two are combined in the lowest curve. (B) Trp-Ala zwitterion (pH 5.5). Components 1–3 are 1.76, 0.313, and 6.47 ns. (C) Ala-Trp anion (pH 9.3). Components 1–3 are 2.74, 0.678, and 2.37 ns. (D) Ala-Trp zwitterion (pH 5.5). Spectral components 1–3 correspond to 1.28, 0.438, and 3.64 ns.

phototube-based fluorometer such as ours, we estimate that a 95% quenched component of correspondingly low intensity would not be distinguishable from noise, especially in the presence of other components.

To make the semantic distinction between this type of quenching and static quenching due to ground-state dark complex formation, we propose that the term *quasi-static self-quenching* (QSSQ). Each component may be dynamically quenched, but a component with a short lifetime and low intensity could go undetected. In our system, $\langle\tau\rangle/Q_{rel}$ rises, indicating QSSQ. Very rapid quenching, indistinguishable from classical static quenching, must be occurring. This suggests that a conformer is present that is largely (if not completely) self-quenched and that interconversion of conformers is slow on the fluorescence time scale. Whether the quenched component truly has a lifetime of zero is unimportant in the context of this study.

Quasi-static quenching is analogous to a functional type of quenching described by Frank and Vavilov (1931). In studying quenching of dyes by iodide, they found that Stern–Volmer plots ($F_0/F$ vs [Q], where $F$ and $F_0$ are the fluorescence intensities in the presence and absence of quencher Q showed upward curvature at higher quencher concentration. This effect was rationalized as due to static quenching that occurred when a quencher molecule is within interaction distance of a fluorophore at the moment of excitation. While plots of $F_0/F$ are nonlinear, of $\tau_0/\tau$ vs [Q] remain linear if the mean lifetimes are used (Eftink & Ghiron, 1980, 1981). While simple kinetic analysis is consistent with static quenching, the presence of highly quenched species with very short lifetimes has been found (Lakowicz et al., 1986).

(*6*) *Energy Transfer in Trp-Trp.* This dipeptide has two potential emitting residues, but we find that all the fluorescence parameters are like those of the Trp in a typical X-Trp dipeptide. For zwitterionic Trp-Trp the emission is not blue-shifted, the decay curve is grossly nonexponential (Figure 5C), the lifetime is short (Table III), and the quantum yield is low (Table IV). The lifetimes of Trp-Trp have been included in the tables for both X-Trp and Trp-X (Table IV) to facilitate comparison. Anionic Trp-Trp has a mean lifetime of 3.05 ns, which is in the range of the lifetimes of X-Trp anions (Table III) but shorter than those of any Trp-X examined (Table II). Similarly, the lifetime of the zwitterion, 1.43 ns, is shorter than any Trp-X lifetime but about average for X-Trp zwitterions. If emission from the N-terminal Trp persisted to any significant extent, energy transfer to the other Trp would have been detected for the following reason: A case of energy transfer where donor and acceptor both emit qualifies as a two-state excited-state reaction system, as defined by Laws and Brand (1979). They showed that both donor and acceptor fluorescences often will contain identical lifetime components that have preexponentials that are equal but opposite in sign. No such negative preexponential was detected in Trp-Trp emission, suggesting that the N-terminal Trp is essentially completely quenched by energy transfer.

Energy transfer is more efficient from N- to C-terminal Trp for several reasons. The longer lifetime of Trp at the amino end can be thought of as increasing the critical distance $R_0$ for energy migration (Förster, 1947), thus increasing the transfer efficiency. In the zwitterionic form, the blue shift of the potential emission from the N-terminal Trp increases its overlap with the absorption band of the C-terminal Trp. Conversely, the blue shift of the absorption due to the N-terminal Trp reduces transfer efficiency to it. Wiget and Luisi

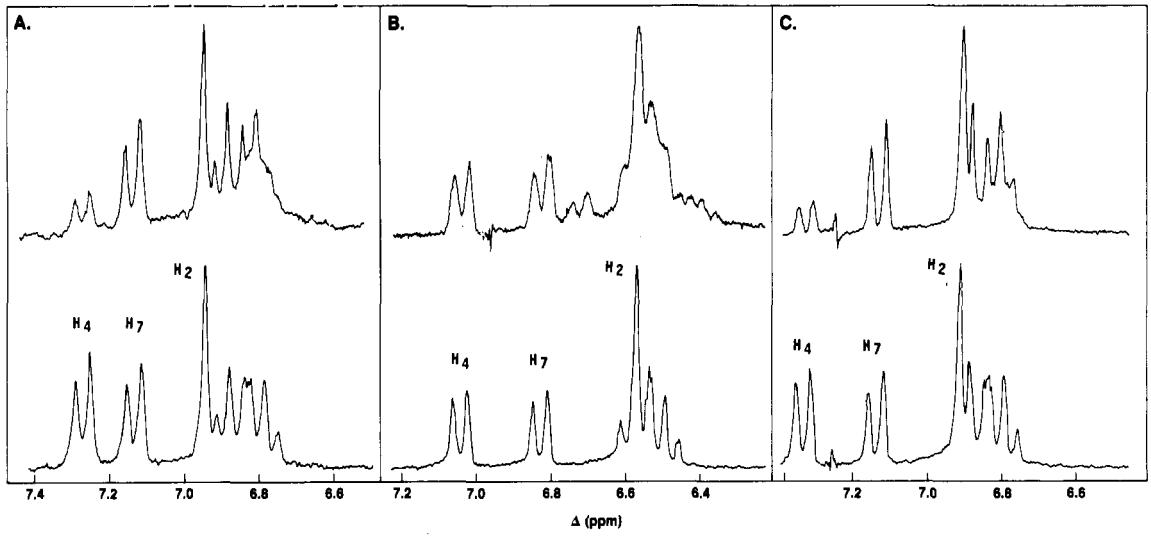


FIGURE 7: NMR spectra of photochemical H–D-exchange experiment. The aromatic regions are shown for (A) tryptophan, (B) Ala-Trp, and (C) Trp-Ala before (lower spectrum) and after (upper spectrum) irradiation. The concentrations were 10 mg/mL in $D_2O$, and exposure to the high-pressure xenon arc was performed as described under Materials and Methods.

(1978) have examined the absorption and emission spectra and quantum yield of Trp-Trp as a function of pH. They found that the absorption maximum of the zwitterion was intermediate between that of Gly-Trp and Trp-Gly and that the quantum yield was lower than expected, i.e., not intermediate between those of peptides containing N-terminal and C-terminal Trps. Their reported $pK_a$ of 7.3 is consistent with the 7.18 found by us. Their results can be interpreted as follows: Each Trp exhibited independent absorption of light, but the emission properties are consistent with our interpretation that only the C-terminal Trp emits.

(7) *Photochemical H–D Exchange.* Saito and co-workers (1984, 1985) showed that the amino group of tryptophan was close to C-4 of the indole moiety by demonstrating that the proton at C-4 exchanged with a deuteron when a $D_2O$ solution of tryptophan was irradiated. They followed the reaction by $^1H$ NMR, where the C-4 proton appears at lowest field. We have duplicated their results with tryptophan and also examined the behavior of *N*-methyltryptophan, *N*,*N*,*N*-trimethyltryptophan, Ala-Trp, Trp-Ala, Leu-Trp, and Trp-Leu under similar reaction conditions. The irradiation of the dipeptides was performed at pD 5.5, while irradiation of *N*-methyltryptophan and tryptophan was carried out at pD 7.0. We found that exchange occurred in tryptophan, its *N*-methyl derivative, Trp-Ala, and Trp-Leu, but no exchange was found for the trimethyl derivative, Ala-Trp, or Leu-Trp. Figure 7 shows NMR spectra for such an experiment. Exchange is evidenced in tryptophan and Trp-Ala by the striking decrease, upon irradiation, of the H-4 resonance relative to H-7. In Ala-Trp, photodegradation is evident, but the relative heights of the H-4 and H-7 regions are unchanged with irradiation.

## Discussion

(1) *Characteristics of Tryptophanyl Rotamers.* The nonexponential decay of tyrosyl derivatives was explained by Gauduchon and Wahl (1978) as due to the presence of conformers formed by rotation about the $C_\alpha$–$C_\beta$ carbon bond. This rotamer model was adopted by Szabo and Rayner (1980) to explain the nonexponential decay of tryptophan. The work of Chang et al. (1983) and Petrich et al. (1983) extended the rotamer model to other indole derivatives and tried to correlate structure with the degree of nonexponentially. It has been pointed out (Gudgin-Templeton & Ware, 1984) that all attempts to assign rotamer populations on the basis of fluorescence decay data have been inconsistent with NMR studies. More recently, it has been reported that molecular dynamics simulations show that $C_\alpha$–$C_\beta$ rotamers interconvert rapidly and that there was a better correlation between fluorescence decay and rotamers formed by rotation about the $C_\beta$–$C_\gamma$ bond (Engh et al., 1986). The lifetime data would seem to require different conformers that interconvert slowly relative to the fluorescence time scale, but whether there are only a few conformers (rotamers) or many is still unsettled. Fluorescence decay data can be analyzed according to a model of a polymodal distribution of lifetimes (James & Ware, 1985, 1986), so that it is not a priori evident whether there are a few or many emitting species. Such a distinction probably cannot be made without global analysis of many data sets (Knutson et al., 1983).

In the present study, we analyzed fluorescence decays of Trp dipeptides according to a triple-exponential model and combined these results with other physical measurements to see if the data correlated with the presence of a few or many slowly interconverting conformers. As discussed further below, the results are consistent with Trp-X zwitterion being dominated by a rotamer with the $-NH_3^+$ group near the indole, while X-Trp zwitterions exhibit static quenching, suggesting close proximity of the indole and the peptide carbonyl in a significant fraction of the molecules. These results are most easily explained by the presence of a few discrete rotamers. On the other hand, the anionic forms of the Trp dipeptides exhibit much more exponential fluorescence decay, which is not inconsistent with rapid interconversion of conformers. It would be speculative to say that the same conformers present in the zwitterions persist in the anions.

(2) *Indole Interaction with the $-NH_3^+$ Group in Trp-X Rotamers.* The data are in accord with the classic model of three rotamers formed by rotation about the $C_\alpha$–$C_\beta$ bond, as shown in Figure 8 for Trp dipeptides. For Trp-X, rotamer I (Figure 8A) is favored sterically, and is consistent with data showing that the indole is near the $-NH_3^+$ group. Such proximity is required for the photochemical H–D exchange, the blue shifts in both absorption and emission, and the increased acidity of the $-NH_3^+$ group. The relatively high quantum yield of Trp-X zwitterion is also consistent with this proximity as the $-NH_3^+$ group is a weak quencher (Cowgill, 1967). The decay kinetics and DAS for Trp-X suggest that one rotamer dominates. The spectral shifts for tryptophan and Trp-Gly were also noted by Wiget and Luisi (1978) and Chang et al. (1983). The present study shows that this phenomenon

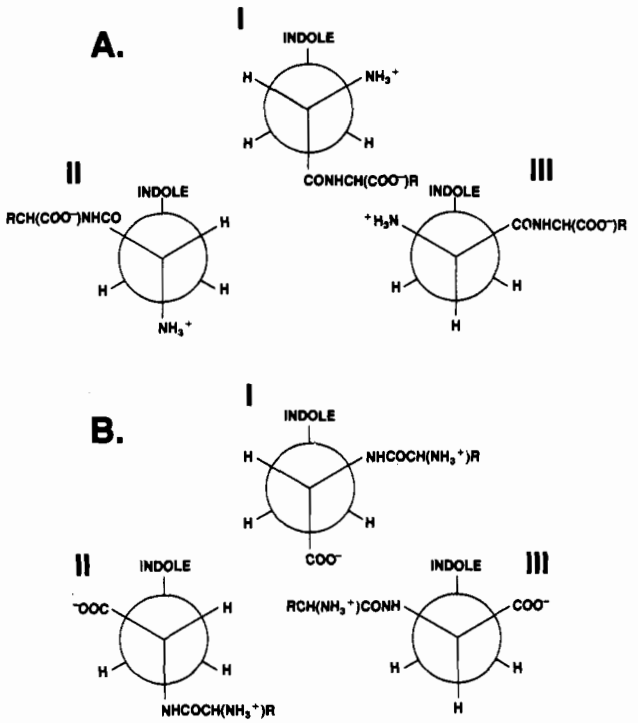


FIGURE 8: Rotamer models (Newman projections) for Trp-X (A) and X-Trp (B) dipeptides based on rotation about the $C_\alpha$–$C_\beta$ bond.

is general for Trp-X dipeptides. Protonation of the amino group causes an emission blue shift of approximately 10 nm for all Trp-X peptides we have examined except Trp-Trp, which is discussed below. We have also observed that the emission maximum of *N,N,N*-trimethyltryptophan is the same as that of zwitterionic tryptophan or Trp-X, showing that it is the charge rather than the proton that causes the blue shift. In proteins, a blue-shifted fluorescence spectrum is generally attributed to tryptophan in a protected environment, such that dipole relaxation is minimal during the excited state. In view of the present findings, one must also consider a nearby positively charged group as a possible factor causing a blue shift. In proteins, the magnitude of the blue shift could depend on the nearness of the indole group to a positive charge as well as the relative proportions of different rotamers. Tryptophan peptides were titrated in order to find the pH ranges where the anions and zwitterions predominate, but the p$K_a$ data also permit structural inferences. The p$K_a$ values for Trp-X dipeptides are lower than those of X-Trp by 0.3–0.4 unit, with the exception of the case where X = Phe. The effect may be attributed to the indole group being closer to the $-NH_3^+$ group in Trp-X than in X-Trp. The hydrophobic group can be viewed as stabilizing the uncharged amino group resulting from deprotonation. The lower p$K_a$ of Phe–Trp compared with that of Trp-Phe is explained by the lower polarity of the phenyl group compared with that of the indole moiety. The p$K_a$ values of Phe-Trp and Trp-Phe, 6.75 and 6.92 (Table I), are both lower than those of any other dipeptide examined, indicating that the effects of the hydrophobic groups are additive. The values are slightly lower than the p$K_a$ of Trp-Trp, 7.18, again indicating the greater hydrophobicity of Phe over Trp.

Literature values of p$K_a$ for dipeptides are in the range of 7.9–8.2, while those of free amino acids range from about 9.3 to 9.7 (Martell & Smith, 1974). The p$K_a$ values we find for Trp-X and X-Trp dipeptides are generally lower than those of nonaromatic dipeptides such as Ala-X and Gly-X (Perkins, 1954). This suggests that Trp at either position tends to lower the p$K_a$. However, in β-Ala-Trp the amino group is relatively distant from the indole and the p$K_a$ is found to be 9.08 (Table I). Chang et al. (1983) obtained p$K_a$ values for Trp-Gly (7.79) and Trp-Ala (7.86) that are higher than ours: 7.53 and 7.32, respectively (Table I). However, our values for Trp-Gly, Gly-Trp, and Trp-Trp are within 0.1 unit of those reported by Wiget and Luisi (1978). Our value of 7.93 for the p$K_a$ of Gly-Trp is in good agreement with the value of 8.04 obtained by Perkins (1954) using potentiometric titration under slightly different ionic strength conditions.

The good agreement between p$K_a$ values obtained by fluorescence and absorption methods indicates absence of excited-state proton effects, which would be unlikely since the amino group is not attached to the indole.

The choice of pH 5.5 to examine peptide zwitterions represents a compromise to minimize the contributions of the cationic and anionic forms, but it should be recognized that there is no pH where these contributions are entirely absent. At pH 5.5 for the peptides listed in Table I, the conversion of anion to zwitterion is ≥98% except for Phe-Trp (94%) and Trp-Phe (96%). Relatively little of the cation occurs at pH 5.5 as the p$K_a$ of the carboxyl group in tryptophan peptides ranges from 2.4 to 3.4 (Wiget & Luisi, 1978). On the other hand, the p$K_a$ of many Trp-X dipeptides is near 7, so that some anion is present at pH 5.5. (Because of their high p$K_a$ values, β-Ala-Trp and Pro-Trp anions were measured at pH 10.) In assessing the fluorescence decay data, one should recall this lack of ionic purity, which in the case of Trp-X zwitterions may contribute to the deviation from monoexponential decay and the low $\langle\tau\rangle$ values, as indicated above.

Data on Trp dipeptides obtained at pH 7 arise from both the anionic and zwitterionic forms since, as we show, the p$K_a$ values are between 7 and 8. For this reason, such data are hard to evaluate; examples include the quantum yields reported by Cowgill (1967) for Gly-Trp, Trp-Gly, Leu-Trp, and Trp-Leu and the lifetime data of Ross et al. (1981) on Gly-Trp and Trp-Gly.

The reciprocal effects of the $-NH_3^+$ and indole groups indicate that these two groups are in proximity in Trp-X and tryptophan. Of the rotamers in Figure 8A, I and III fulfill this requirement, although the former is more favored sterically. This conclusion is in contrast to the structures suggested for tryptophan, whose fluorescence decay has a major component of 3.10 ns and a minor, subnanosecond component (Raynor & Szabo, 1978). Gudgin-Templeton and Ware (1984) postulated that the major lifetime component was due to the rotamer with indole closest to the $-COO^-$ group (rotamer II of Figure 8A), while the short lifetime component was assigned to a rotamer with indole near the $-NH_3^+$ group. Our assignment of structure I as the major rotamer is consistent with the relatively high quantum yields and long lifetimes of Trp-X dipeptides since the $-NH_3^+$ group is not in itself a strong quencher (Cowgill, 1967), although it can potentiate carbonyl quenching.

(*3*) *Statistically Self-Quenched Rotamers of Tryptophanyl Peptides.* The data of Table IV show large differences in the ratios of lifetime/quantum yield. These differences could arise (a) if the natural lifetimes $\tau_n$ differed or (b) if static quenching were present. Let us consider these two possibilities.

(*a*) *Change in Radiative Lifetimes.* Equations for the calculation of the natural, or radiative, lifetime $\tau_n$ have been derived by Förster (1950) and refined by Strickler and Berg (1962) and Birks and Dyson (1964). Such calculation is based on the electronic spectra of the emitting transition, and this general approach has been validated experimentally by Birks and Munro (1966) for compounds having mirror symmetry

of the absorption and emission bands. Application of these equations to indole derivatives is not straightforward because of the lack of mirror symmetry, which is due to a complex absorption spectrum containing overlapping $^1L_b$ and $^1L_a$ bands. Nevertheless, the radiative lifetimes $\tau_n$ of indoles would be expected to be closely tied to their spectra. Moreover, when the $^1L_a$ band is resolved (Valeur & Weber, 1977), it is seen to be symmetric with the emission, which is also due to this transition. Since the indole compounds studied here have very similar absorption and emission spectra, they should also have similar radiative lifetimes.

Radiative lifetimes of indole derivatives have been shown to vary with solvent (Privat et al., 1979). However, these changes were accompanied by changes in spectra caused by association of the compounds with solvent molecules (Walker et al., 1971). Another possible cause of a change in radiative lifetimes of indoles could be a change in the emitting state. Indoles generally emit from the $^1L_a$ state in polar solvents (Creed, 1984), but emission from the $^1L_b$ state has been observed in certain indoles in organic solvents at low temperature (Strickland & Billups, 1973; Song & Kurtin, 1969; Valeur & Weber, 1977). Under any conditions, it is unlikely that there would be a change in the emitting state, without significant spectral change.

One concludes that the differences in lifetime/quantum yield ratios cannot be explained by differences in radiative lifetime.

(*b*) *The Question of Static Quenching in Trp Derivatives.* After measuring the fluorescence decay kinetics and quantum yields of the anionic and zwitterionic forms of Trp dipeptides, we conclude that some compounds exhibit quasi-static self-quenching (QSSQ) because the lifetime/quantum yield ratios are larger than expected. These compounds have very similar absorption and emission spectra and the deviations of $\langle\tau\rangle/Q_{rel}$ from a common value were large enough that QSSQ is most probable. A few other reports of possible static self-quenching in Trp derivatives have appeared. Werner and Forster (1979) found that Pro-Trp exhibited an anomalously high $\langle\tau\rangle/Q_{rel}$ value and suggested that there might be static quenching. More recently, static quenching has been implicated by Szabo (1988) in Lys-Trp-Lys and the peptide bombesin.

Several aspects of the data presented here suggest that QSSQ may not be as rare as suggested by the paucity of such reports. First, our measurements show that Leu-Trp, Lys-Trp, and Pro-Trp zwitterions have $\langle\tau\rangle/Q_{rel}$ values greater than 3.8, while simpler indoles such as *N*-acetyltryptophan have ratios near 2.5–2.6. Second, the lifetime/yield ratios of the anions of the X-Trp dipeptides studied are generally lower than those of the corresponding zwitterions. Third, while other studies have shown that many indole derivatives have lifetime/yield ratios consistent with that of tryptophan (Werner & Forster, 1979; Chang et al., 1983; Petrich et al., 1983), tryptophan zwitterion may exhibit QSSQ. As noted before, $\langle\tau\rangle/Q_{rel}$ was significantly higher for Trp than for *N*-acetyltryptophan: 3.1 vs 2.5. This difference is outside of experimental error for the following reasons: In determining the quantum yield, we measured each optical density and fluorescence intensity five times in order to calculate the relative yield $Q_{rel}$. The standard deviations were 1.1–3.0% of the mean. Repeated determinations of mean lifetimes fell within 2% of the mean. Therefore, differences in $\langle\tau\rangle/Q_{rel}$ greater than about 6% are probably real.

In the past, problems with precision may have precluded the finding of static self-quenching. Ricci (1974) and Ricci and Nesta (1976) attempted similar comparisons with a lifetime apparatus associated with variations of ±0.5 ns for compounds whose lifetimes were in the range of 1–2 ns. The error in lifetime/quantum yield ratios in the work of Werner and Forster (1979) was estimated to be ±15–20%. The error in quantum yields was said to be ±10% in the work of Petrich et al. (1983).

Additional evidence for QSSQ in Trp based on calculations of natural lifetime and comparison with other indoles will be presented elsewhere (Chen, Wong, and Knutson, manuscript in preparation).

The occurrence of QSSQ is correlated with the presence of carbonyl and protonated amino groups and is most prominent in the X-Trp zwitterions. Examination of the Newman projections of Figure 8B reveals that each of the three classical $C_\alpha$–$C_\beta$ rotamers of X-Trp zwitterion can have a carbonyl-containing group near the indole moiety. Rotamer III is not favored sterically, while rotamer I has been shown to bring the peptide carbonyl closest to the indole (Werner & Forster, 1979). Some variation of rotamer I is likely to be the most quenched conformer. (In addition to the classical depictions of Figure 8, different orientations of the indole ring due to rotation about the $C_\beta$–$C_\gamma$ bond yield more conformers.) The difference in fluorescence behavior of X-Trp zwitterions and anions is no doubt due to the influence of the protonated amino group, which potentiates the quenching power of the peptide carbonyl (Cowgill, 1963; Werner & Forster, 1979), thus enlarging its "sphere of interaction".

One might argue that the presence of impurities could lower the quantum yield, thus giving the impression of static quenching. Such an argument could not easily explain the different $\langle\tau\rangle/Q_{rel}$ values at different pH *for the same compound.* An impurity artifact would have to be manifested at pH 5.5 but not at pH 9.3. Also, matched pairs of dipeptides, Trp-X and X-Trp, were examined, and any putative impurities would have to be present only in X-Trp where we find most evidence for QSSQ and not in Trp-X—an unlikely circumstance.

As defined under Results, QSSQ includes weak fluorescence that is not detected. An ideal instrument would measure and quantitate all decay components that are dynamically quenched. For our purposes, the question of whether a component is completely quenched or only 95% quenched is immaterial. The main relevance of QSSQ is that it argues for a self-quenched conformer that interconverts slowly relative to the fluorescence time scale and thus supports the rotamer model.

(*4*) *Extent of QSSQ in Trp Peptides.* The lifetime and quantum yield data of Table IV can be used to estimate the fraction $f_{sq}$ that is subject to QSSQ. Assume the molecular population to consist of one fraction subject to QSSQ and one with a quantum yield, $Q$. If both fractions become identical when QSSQ is eliminated, it follows that

$$f_{sq} = 1 - [\langle\tau\rangle/Q_{rel}]_s/[\langle\tau\rangle/Q_{rel}]_x \quad (4)$$

where the subscripts s and x refer to the values for an indole derivative with no static quenching and the compound under study. The values of $\langle\tau\rangle/Q_{rel}$ for *N*-acetyltryptophan and Leu-Trp at pH 5.5 are 2.5 and 4.55, yielding $f_{sq} = 0.45$. For Lys-Trp and Leu-Trp, $f_{sq}$ is about 0.34. For a compound with a $\langle\tau\rangle/Q_{rel} = 3.0$, $f_{sq} = 0.17$.

It is apparent that QSSQ can affect a significant fraction of molecules that contain both a fluorophore and a strongly quenching function, such as a carbonyl that is potentiated by a nearby protonated amino group. The presence of QSSQ could invalidate attempts to estimate rotamer populations based on fluorescence decay analyses, since some of the molecules do not contribute to the fluorescence.

(*5*) *Quenching by Proton Transfer in Tryptophanyl Rotamers.* A number of quenching mechanisms have been postulated for indoles. Proton transfer to the excited indole, charge (electron) transfer from the indole to an acceptor such as a carbonyl group, photoelectron ejection, intersystem crossing, and internal conversion pathways have been postulated. The extensive literature on the photophysics of indoles including tryptophan derivatives has been reviewed (Santus et al., 1980; Creed, 1984). Saito et al. (1984, 1985) showed that ultraviolet radiation of tryptophan zwitterion in $D_2O$ resulted in H–D exchange at C-4 of the indole ring, with a quantum yield of about 0.14, and that the anion did not exchange. Trp-Tyr was said to show H–D exchange. Shizuka et al. (1988) extended these studies. A crown ether was used to cage the $-NH_3^+$ group of tryptophan zwitterion, resulting in a 3-fold enhancement of fluorescence at room temperature and absence of photochemical H–D exchange. Assuming that the enhancement was due entirely to the effective removal of the $-NH_3^+$ group, they calculated rate constants for quenching by proton transfer from this group. Our results lead to somewhat different conclusions. We found H–D exchange in tryptophan, Trp-X dipeptides, and *N*-methyltryptophan but not in *N*,*N*,*N*-trimethyltryptophan. The photochemical H–D exchange requires both a positive charge and a hydrogen on the amino group, the transferred proton coming directly from the amino group rather than the solvent. Since tryptophan and the trimethyl derivative have similar quantum yields and lifetimes (Table IV), proton transfer would not seem to be a *necessary* mechanism of quenching. The fluorescence enhancement produced by encircling the $-NH_3^+$ with a crown ether (Shizuka et al., 1988) could be at least partly due to the environmental change due to the presence of the large, hydrophobic crown ether resulting in a change in solvent structure around the indole ring.

(*6*) *Conclusions.* These studies have yielded new data on the physical properties of Trp peptides. While the information increases understanding of the intramolecular interactions of the peptides themselves, there is also relevance to protein fluorescence. The blue shift in the emission spectrum of Trp dipeptides in the presence of a nearby charged amino group suggests another basis for blue shifts in tryptophanyl protein spectra. Also, since Trp dipeptide conformers exhibit state self-quenching, the same phenomenon may exist in proteins. Finally, the results are consistent with the presence of rotamers of Trp dipeptides that interconvert slowly relative to the fluorescence time scale, and inferences can be made as to the structures of some of these rotamers.

**Registry No.** Trp, 73-22-3; Ala-Trp, 16305-75-2; Trp-Ala, 24046-71-7; β-Ala-Trp, 21612-37-3; Trp-β-Ala, 67607-64-1; Gly-Trp, 2390-74-1; Trp-Gly, 7360-09-0; Gly-Gly-Trp, 20762-32-7; Trp-Gly-Gly, 20762-31-6; Leu-Trp, 5156-22-9; Trp-Leu, 13123-35-8; Phe-Trp, 24587-41-5; Trp-Phe, 6686-02-8; Trp-Trp, 20696-60-0; Val-Trp, 24587-37-9; Trp-Val, 24613-12-5; Pro-Trp, 35310-39-5; Trp-Ser, 133101-40-3; Trp-Glu, 36099-95-3; Trp-Lys, 51790-14-8; Trp-Tyr, 19653-76-0; N-Ac-Trp, 1218-34-4; Glu-Trp, 38101-59-6; Lys-Trp, 2390-74-1; Tyr-Trp, 60815-41-0.

## REFERENCES


Badea, M. G., & Brand, L. (1979) *Methods Enzymol. 61*, 378–425.

Beechem, J. M., & Brand, L. (1985) *Annu. Rev. Biochem. 54*, 43–71.

Birks, J. B., & Dyson, D. J. (1963) *Proc. R. Soc. London A275*, 135–148.

Birks, J. B., & Munro, I. H. (1967) in *Progress in Reaction Kinetics* (Porter, G., Ed.) Vol. 4, pp 239–304, Pergamon Press, London.

Chang, M. C., Petrich, J. W., McDonald, D. B., & Fleming, G. R. (1983) *J. Am. Chem. Soc. 105*, 3819–3824.

Chen, R. F. (1967) *Anal. Lett. 1*, 35–42.

Chen, R. F., & Knutson, J. R. (1988) *Anal. Biochem. 172*, 61–77.

Chen, R. F., Edelhoch, H., & Steiner, R. F. (1969) in *Physical Principles and Techniques of Protein Chemistry, Part A* (Leach, S. J., Ed.) pp 171–244, Academic Press, New York.

Conti, C., & Forster, L. S. (1975) *Biochem. Biophys. Res. Commun. 65*, 1257–1263.

Cowgill, R. W. (1963) *Arch. Biochem. Biophys. 100*, 36–44.

Cowgill, R. W. (1967) *Biochim. Biophys. Acta 133*, 6–18.

Creed, D. (1984) *Photochem. Photobiol. 39*, 534–562.

DeLauder, W. B., & Wahl, P. (1971) *Biochem. Biophys. Res. Commun. 42*, 398–404.

Dezube, B., Dobson, C. M., & Teague, C. E. (1981) *J. Chem. Soc., Perkin Trans. 2*, 730–736.

Eftink, M. R., & Ghiron, C. A. (1980) *J. Phys. Chem. 80*, 486–493.

Eftink, M. R., & Ghiron, C. A. (1981) *Anal. Biochem. 114*, 199–227.

Engh, R. A., Chen, L. X.-Q., & Fleming, G. R. (1986) *Chem. Phys. Lett. 126*, 365–372.

Fleming, G. R., Morris, J. M., Robbins, R. J., Woolfe, G. J., Thistlewaite, P. J., & Robinson, G. W. (1978) *Proc. Natl. Acad. Sci. U.S.A. 75*, 4652–4656.

Formoso, C., & Forster, L. S. (1975) *J. Biol. Chem. 250*, 3738–3745.

Förster, Th. (1951) *Fluoreszenz Organische Verbindungen*, Vandenhoek u. Ruprecht, Gottingen.

Frank, I. M., & Vavilov, S. (1931) *Z. Phys. 69*, 100–110.

Gauduchon, P., & Wahl, P. (1978) *Biophys. Chem. 8*, 87–104.

Grinvald, A., & Steinberg, I. Z. (1974) *Anal. Biochem. 59*, 583–598.

Grinvald, A., & Steinberg, I. Z. (1976) *Biochim. Biophys. Acta 427*, 663–678.

Gudgin, E., Lopez-Delgado, R., & Ware, W. R. (1981) *Can. J. Chem. 59*, 1037–1044.

Gudgin-Templeton, E. F., & Ware, W. R. (1984) *J. Phys. Chem. 88*, 4626–4631.

Hermans, J., Jr., Donovan, J. W., & Sheraga, H. A. (1960) *J. Biol. Chem. 235*, 91–93.

James, D. R., & Ware, W. R. (1985) *Chem. Phys. Lett. 120*, 455–459.

James, D. R., & Ware, W. R. (1986) *Chem. Phys. Lett. 126*, 7–11.

Knutson, J. R., Walbridge, D. G., & Brand, L. (1982) *Biochemistry 21*, 4671–4679.

Knutson, J. R., Beechem, J. M., & Brand, L. (1983) *Chem. Phys. Lett. 102*, 501–507.

Lakowicz, J. R., Johnson, M. L., Joshi, N., Gryczynski, I., & Laczko, G. (1986) *Chem. Phys. Lett. 131*, 343–348.

Laws, W. R., & Brand, L. (1979) *J. Phys. Chem. 83*, 795–802.

Laws, W. R., Ross, J. B. A., Wyssbrod, H. R., Beecham, J. M., Brand, L., & Sutherland, J. C. (1986) *Biochemistry 25*, 599–607.

Parker, C. A., & Rees, W. T. (1960) *Analyst 85*, 587–600.

Perkins, D. J. (1954) *Biochem. J. 57*, 702–704.

Petrich, J. W., Chang, M. C., McDonald, D. B., & Fleming, G. R. (1983) *J. Am. Chem. Soc. 105*, 3824–3832.

Pringsheim, P. (1949) *Fluorescence and Phosphorescence*, Interscience Publishers, Inc., New York.

Privat, J.-P., Wahl, P., & Auchet, J.-C. (1979) *Biophys. Chem. 9*, 223–233.

Rayner, D. M., & Szabo, A. G. (1978) *Can. J. Chem. 56*, 743–745.
Ricci, R. W. (1974) *Photochem. Photobiol. 12*, 67–75.
Ricci, R. W. & Nesta, J. M. (1976) *J. Phys. Chem. 80*, 974–980.
Robbins, R. J., Fleming, G. R., Beddard, G. S., Robinson, G. W., Thistlewaite, P. J., & Woolfe, G. J. (1980) *J. Am. Chem. Soc. 102*, 6271–6279.
Ross, J. B. A., Rousslang, K. W., & Brand, L. (1981) *Biochemistry 20*, 4361–4369.
Ross, J. B. A., Laws, W. R., Buku, A., Sutherland, J. C., & Wyssbrod, H. R. (1986) *Biochemistry 25*, 607–612.
Saito, I., Sugiyama, H., Yamamoto, A., Muramatsu, S., & Matsuura, T. (1984) *J. Am. Chem. Soc. 106*, 4286–4287.
Saito, I., Muramatsu, S., Sugiyama, H., Yamamoto, A., & Matsuura, T. (1985) *Tetrahedron Lett. 26*, 5891–5894.
Santus, R., Bazin, M., & Aubailly, H. (1980) *Rev. Chem. Intermed. 3*, 231–283.
Shizuka, H., Serizawa, M., Shimo, T., Saito, I., & Matsuura, T. (1988) *J. Am. Chem. Soc. 110*, 1930–1934.
Song, P. S., & Kurtin, W. E. (1969) *Photochem. Photobiol. 9*, 175–178.
Strickland, E. H., & Billups, C. (1973) *Biopolymers 12*, 1989–1995.
Szabo, A. G. (1989) in *The Enzyme Catalysis Process: Energetics, Mechanism, and Dynamics* (Cooper, A., Houben, J. L., & Chien, L. C., Eds.) pp 123–139, Plenum Press, New York.
Szabo, A. G., & Rayner, D. M. (1980) *J. Am. Chem. Soc. 102*, 554–563.
Valeur, B., & Weber, G. (1977) *Photochem. Photobiol. 25*, 441–444.
Walker, M. S., Bednar, T. W., Lumry, R., & Humphries, F. (1971) *Photochem. Photobiol. 14*, 147–161.
Ware, W. R., & Nemzek, T. L. (1975) *J. Chem. Phys. 62*, 477–489.
Werner, T. C., & Forster, L. S. (1979) *Photochem. Photobiol. 29*, 905–914.
Wiget, P., & Luisi, L. (1978) *Biopolymers 17*, 167–180.

# Physicochemical Properties of Cloned Nucleocapsid Protein from HIV. Interactions with Metal Ions†

Daniel W. Fitzgerald‡ and Joseph E. Coleman*
*Department of Molecular Biophysics and Biochemistry, Yale University, New Haven, Connecticut 06510*
*Received December 18, 1990; Revised Manuscript Received February 19, 1991*

ABSTRACT: The nucleocapsid (NC) protein (p15) of the human immunodeficiency virus (HIV) has been cloned and overproduced (under the control of a phage T7 promoter) in soluble form in an *Escherichia coli* host. The soluble NC protein is a fusion protein containing 15 amino acids from the T7 gene 10 and 7 amino acids from the HIV p24 protein at the N-terminus to make a protein of 171 amino acids. The plasmid containing the fusion gene is designated p15DF. A homogeneous product has been isolated from the induced cells and, when isolated under aerobic conditions, contains 0.3–0.5 mol of Zn/mol of protein and has only 2 titratable SH groups. Reduction and refolding in the presence of Zn(II) yields a protein containing 2.0 mol of Zn/mol of protein and 6 titratable SH groups. On the other hand, if the cells are sonicated in 2 mM $CdCl_2$ and purified at pH 5.0, an unoxidized protein containing 2 mol of Cd/mol of protein is obtained. The Cd(II) ions can be exchanged with Zn(II), Co(II), or $^{113}$Cd(II). The $Co(II)_2$ NC protein shows d–d electronic transitions at 695 nm [$\epsilon$ = 675 $M^{-1}$ $cm^{-1}$ per Co(II)] and 640 nm [$\epsilon$ = 825 $M^{-1}$ $cm^{-1}$ per Co(II)] compatible with regular tetrahedral geometry around both Co(II) ions. The $Co(II)_2$ and $Cd(II)_2$ NC proteins show intense charge-transfer bands in the near-UV, at 355 nm ($\epsilon$ = ~4000 $M^{-1}$ $cm^{-1}$) and 310 nm ($\epsilon$ = ~8000 $M^{-1}$ $cm^{-1}$) for the Co(II) protein and 255 nm ($\epsilon$ = ~$10^4$ $M^{-1}$ $cm^{-1}$) for the $Cd(II)_2$ NC protein, compatible with $-S^-$ coordination. $^{113}$Cd NMR of the $^{113}Cd(II)_2$ NC protein shows two $^{113}$Cd NMR signals at 659 and 640 ppm, respectively, each integrating to ~1 Cd(II) ion. The downfield chemical shifts suggest coordination of each $^{113}$Cd(II) ion to 3 sulfur donor atoms. The spectroscopic data fully support the prediction that the NC protein binds metal ions to each of the tandem repeats of the -Cys-$X_2$-Cys-$X_4$-His-$X_4$-Cys- sequence contained in the N-terminal half of the molecule. $^{113}$Cd NMR shows, however, that the sites are not identical. Isolation of the NC protein under standard aerobic conditions results in oxidation of the sulfhydryl groups and loss of the coordinated Zn(II) ions, while preparation of the NC protein as the Cd(II) derivative at low pH protects the sulfhydryl groups from oxidation.

The nucleocapsid protein (NC) of the human immunodeficiency virus (HIV), also known as p15, is a protein of 149 amino acids and is coded for by the 3′-end of the GAG gene of the AIDS virus, HIV (Ratner et al., 1985; Guyader et al., 1987). The GAG gene product, a polyprotein, is transported to the cell membrane and incorporated into the budding viral particle where it is subsequently cleaved by the viral-encoded protease into three major polypeptides, the NC protein being released from the C-terminal portion of the polyprotein. There appears to be further cleavage of a portion of the NC protein into two smaller products, p7 and p9 (Veronese et al., 1987; Mervis et al., 1988; Henderson et al., 1988), but the functional

† This work was supported by NIH Grants GM21919 and DK09070. The 500-MHz NMR was supported by NIH Grant RR03475, NSF Grant DMB-8610557, and ACS Grant RD259.
* Corresponding author.
‡ Supported in part by NIH Cancer Education Grant R25-CA47883.

0006-2960/91/0430-5195$02.50/0 